Available online at www.sciencedirect.com
ScienceDirect
Dyes and Pigments 77 (2008) 678–685
DYES and PIGMENTS
www.elsevier.com/locate/dyepig

The synthesis and optical properties of three stilbene-type dyes

Chuanxiang Qin, Maoyi Zhou, Weizhou Zhang, Xiaomei Wang, Guoqiang Chen*

College of Material Science and Engineering, Soochow University, Suzhou 215021, China

Received 30 March 2007; received in revised form 30 June 2007; accepted 5 July 2007
Available online 7 August 2007

Abstract

Three "D–π–A" stilbene-type dyes, namely *trans*-4-[*p*-(*N*,*N*-di (2-hydroxyethyl))-amino-styryl]-*N*-methyl pyridinium iodide (DHEASPI-C_1), *trans*-4-[*p*-(*N*,*N*-di (2-hydroxyethyl))-amino-styryl]-*N*-octyl pyridinium bromide (DHEASPBr-C_8) and *trans*-4-[*p*-(*N*,*N*-di (2-hydroxyethyl))-amino-styryl]-*N*-dodecyl pyridinium bromide (DHEASPBr-C_{12}) were synthesized and their optical properties in different environments were investigated. Red shifts occurred in both the one-photon and two-photon fluorescence spectra from DHEASPI-C_1 to DHEASPBr-C_8 and to DHEASPBr-C_{12} as the alkyl group in the terminal acceptor was changed from methyl through octyl to dodecyl. When a 1064 nm, <130 fs mode-locked Nd: YAG laser pulse was pumped, their lasing locations occurred at 613–624 nm. When DHEASPI-C_1 was used as reference, the two-photon absorption cross-sections (σ_s) of DHEASPBr-C_8 and DHEASPBr-C_{12} were 8.02 and 13.5, respectively.
© 2007 Published by Elsevier Ltd.

Keywords: Optical material; Two-photon excited fluorescence; Environment effect

1. Introduction

There is still a growing interest in organic chromospheres with large two-photon absorption (TPA) cross-section and excellent up-conversion emission properties due to their potential for application in a wide range of areas such as frequency-up-converted lasing [1–3], two-photon photodynamic therapy [4], optical-limiting [5], 3-D optical data storage [6–8], etc. Although a lot of TPA active dyes have been synthesized, the structure–property relationship of materials with large TPA cross-section has not been well understood yet, which limits, more or less, the two-photon process applications. At present, numerous organic compounds have been investigated to determine that relationship [9–16], which will help to optimize the choice of applications of oriented molecules. Among lots of compounds with good TPA properties, certain asymmetric substituted Donor–π–Acceptor (D–π–A) type dyes have been investigated by many laboratories [3,17,18]. Prasad et al. revealed that substituted styryl-pyridinium compounds have good two-photon pumped (TPP) properties, and the net conversion efficiency from the absorbed 800 nm pump pulse energy to the ~543 nm unconverted cavity lasing energy was found to be as high as ~11% [3]. In recent years, substituted styryl-pyridinium salts, which can generate larger intra-molecular charge shift, are also an investigation part of Jiang's research group while they laid stress on the planarity of π-center and donor–acceptor strength [19–22]. The influence of donor strength upon TPP emission behavior shows the variety, the charge density distribution and bond length alternation (BLA) [19]. The central wavelength of TPP lasing has largely been influenced by the π-conjugated dye cation, whereas the anion has contribution to enhancing the TPP lasing efficiency [21]. However, when these types of dyes were blended with polymer, the compatibility is inferior and the blending ratio of dyes is minor.

We added the number of hydroxyl of donor group for the purpose of the future graft reaction to manufacture polymer material, while the alkyl group of dyes was changed in their terminal acceptor from methyl to octyl and to dodecyl for their good compatibility with polymer. The results showed that the compatibility with polymer became better as the length of

* Corresponding author. Tel.: +86 512 67162216; fax: +86 512 67246786.
E-mail addresses: xmwangsuda@sohu.com.cn (X. Wang), chenguojiang@suda.edu.cn (G. Chen).

0143-7208/$ - see front matter © 2007 Published by Elsevier Ltd.
doi:10.1016/j.dyepig.2007.07.016

alkyl group increased. Interestingly, we also found that the fluorescence quantum yield (Φ_f) decreased in DMF solution, but the two-photon absorption cross-section (σ_s) increased at the same time. Meanwhile, molecular environment effects are also systematically examined.

2. Experimental

2.1. Instrumental measurement

IR spectra were measured on a Nicolet FT-IR 5DX instrument using solid samples dispersed in KBr disks. Hydrogen nuclear magnetic resonance spectra were determined on a GCT-TOF NMR spectrometer (400 MHz). The melting points and decomposition temperatures were measured on a Perkin Elmer Diamond 5700 thermo-gravimetric analyzer at a heating rate of 20 °C/min under nitrogen atmosphere.

UV–vis absorption spectra of samples were recorded on a TU1800 SPC spectrophotometer with $d_0 = 1.0 \times 10^{-5}$ M in quartz cuvettes of 1 cm path length. Then samples' single-photon fluorescence spectra were measured with the same cell under excitation of the respective maximum absorption wavelength on an Edingburgh 920 fluorophotometer.

For the measurements of the fluorescence quantum yield (Φ_f), 1.0×10^{-5} M dyes were prepared. 4-(Dicyanomethylene)-2-methyl-6-(*p*-(dimethylamino) styryl)-4*H*-pyran (DCM) in THF solution (1.0×10^{-5} M, $\Phi_f = 0.5$) was used as reference and its fluorescence spectrum was obtained by excitation at its absorption maximum at 460 nm. The quantum yield of the tested dye (Φ_{dye}) was calculated using Eq. (1).

$$\Phi_{dye} = \Phi_{ref} \frac{I_{dye} A_{ref}}{I_{ref} A_{dye}} \frac{n_{dye}^2}{n_{ref}^2} \quad (1)$$

where Φ_{ref} (=0.5) and n_{ref} (1.4073) are the fluorescence quantum yield of the reference sample (DCM) in THF and the refractive index of THF solvent, n_{dye} is the refractive index of tested solvent, A_{ref} and A_{dye} are the absorbance values for DCM and tested dye, respectively, I_{ref} and I_{dye} are the areas' integral values of the corrected fluorescence spectra for DCM and tested dye, respectively.

Two-photon absorption cross-section (σ_s) values of dyes in DMF solution were determined using two-photon excited fluorescence (TPEF) method with femtosecond laser pulses. The light source is a mode-locked Nd: YAG laser (1064 nm, <130 fs). Up-converted fluorescence spectra were recorded by a fiber spectrometer (Ocean Optics USB2000 CCD). The concentration of sample in DMF solution is 1×10^{-3} M. The TPA cross-section σ_s of sample is determined by Eq. (2).

$$\sigma_s = \sigma_{ref} \frac{F_s \Phi_{ref} \phi_{ref} C_{ref}}{F_{ref} \Phi_s \phi_s C_s} \quad (2)$$

Here, the subscripts s and ref represent sample and reference molecules, respectively. F is the intensity of the fluorescence signal collected by the fiber spectra meter. Φ_f is the fluorescence quantum yield. ϕ is the overall fluorescence collection efficiency. C is the molar concentration (mol cm^{-3}) of molecules in solution. In this paper, ϕ_{ref} and ϕ_s are considered to be the same because the collection scope of the fiber spectra meter is 1064 nm, which covers emission spectra of samples and reference totally.

2.2. Materials

N-Phenyldiethanolamine was purchased from Acros Organic and used without further purification. Dimethylformamide (DMF), ethanol and methanol were redistilled before use. Other reagents were purchased commercially and used without any further purification. The synthetic procedure is shown in Scheme 1.

2.2.1. Synthesis of 4-(N,N-diethanolanilino) benzaldehyde (compound *3*)

To a flask containing *N*-phenyldiethanolamine (27.19 g, 0.15 mol), acetic anhydride (42.5 mL, 0.45 mol) and pyridine (36.4 mL, 0.45 mol) were added. The mixture was refluxed for 2 h, then cooled and poured into ice water. The resulting mixture was extracted with methylene chloride, washed with water several times, dried with magnesium sulfate and concentrated. The product was purified by column chromatography and yellow viscous oil (compound **1**) was obtained (83%).

In a flask was placed 90 mL of anhydrous dimethylformamide while the flask was cooled in ice bath. Then phosphorus oxychloride (13.8 mL, 0.15 mol) was added dropwise with stirring. After 30 min, compound **1** (33.2 g, 0.125 mol) was added to the flask. The solution was heated at 90 °C for 2 h. The reaction mixture was then cooled and poured over crushed ice in beaker, and neutralized to pH 6–8 by dropwise addition of saturated sodium acetate solution. The mixture was extracted with ethyl acetate. The residue was purified by column chromatography and yellow crystals (compound **2**) with low melting point were obtained (90%).

Within a flask, 12.5 g sodium carbonate was dissolved in 100 mL water, and then compound **2** (32.3 g, 0.11 mol) and 40 mL methanol were added and stirred at reflux temperature for 10 h. The mixture was extracted with ethyl acetate, washed with water several times, dried with magnesium sulfate and concentrated. The product was re-crystallized in ethanol and yellow crystal (compound **3**) was obtained (92%).

*Compound **3***: mp 86 °C. IR (KBr pellet, cm^{-1}): 3381.9 (–OH), 1656.7 (C=O), 1595.7 and 1525.8 (Ar CH), ^{1}H NMR ($CDCl_3$, 400 MHz) δ: 9.69 (1H, –CHO, s), 7.69 (2H, Ar CH, d, *J* 8.8 Hz), 6.72 (2H, Ar CH, d, *J* 8.4 Hz), 3.92 (4H, $-CH_2-$, t, *J* 4.2 Hz), 3.70 (4H, $-CH_2-$, t, *J* 4.6 Hz).

2.2.2. Synthesis of precursors of *1a–1c*

Following Ref. 19, precursors of **1a–1c** were obtained.

A mixture of 9.3 g (0.1 mol) γ-methyl pyridine and 50 mL absolute methanol was added to 0.1 mol halogenated alkane at room temperature. Then the solution was heated at reflux

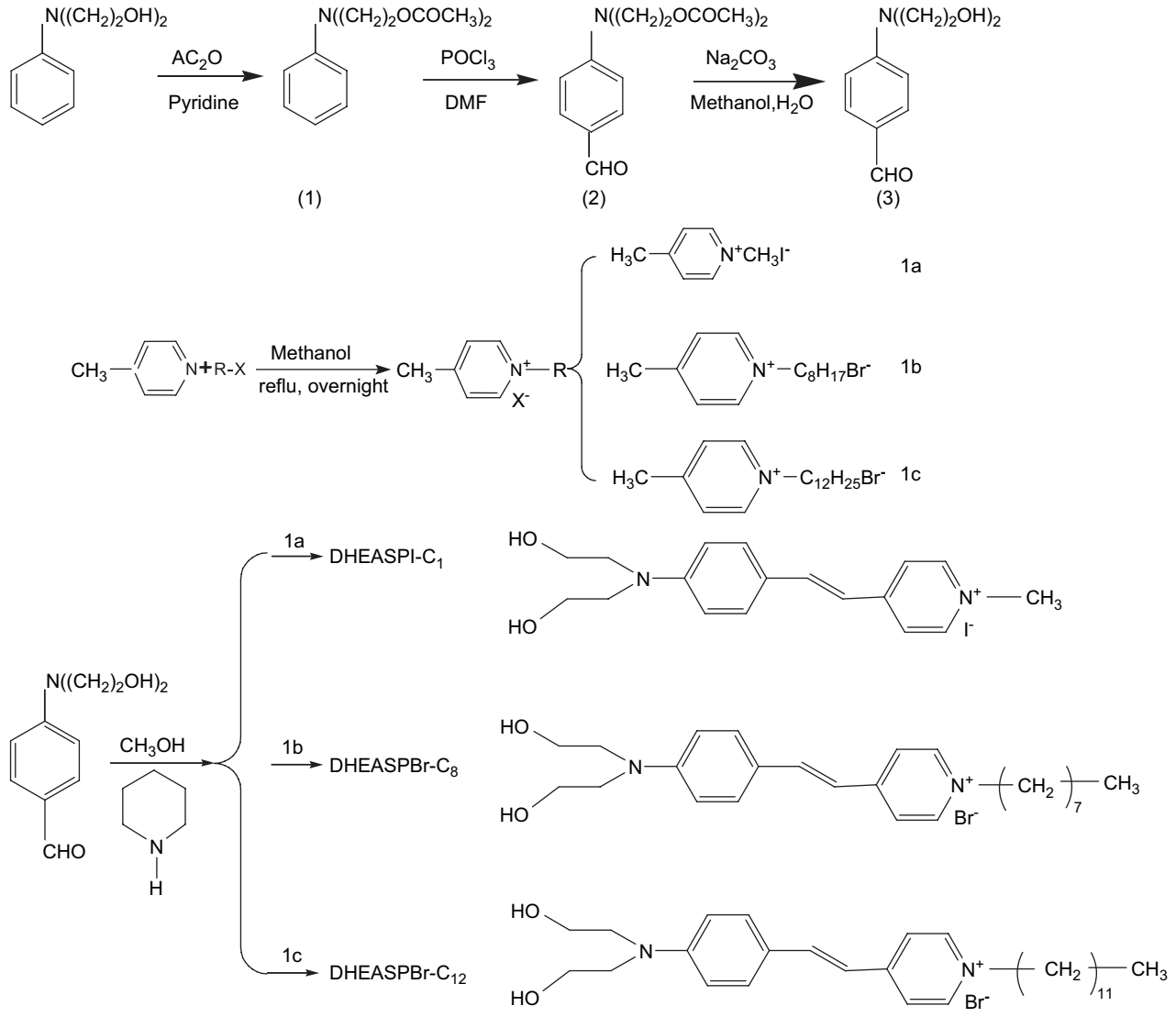

Scheme 1. The synthesis routes of DHEASPI-C_1, DHEASPBr-C_8 and DHEASPBr-C_{12}.

temperature overnight. After the solvent was removed, a white solid was obtained.

*2.2.2.1. 4-Methyl-N-methyl pyridinium iodide (**1a**).* Yield 85% and mp 156 °C. IR (KBr pellet, cm^{-1}): 1643.8 and 1475.7 (Ar CH and CN), ^1H NMR ($CDCl_3$, 400 MHz) δ: 9.17 (d, 2H, Py CH, *J* 6.4 Hz), 7.90 (d, 2H, Py CH, *J* 6.0 Hz), 4.64 (s, 3H, $-CH_3$), 2.70 (s, 3H, CH_3-).

*2.2.2.2. 4-Methyl-N-n-octyl pyridinium bromide (**1b**).* Yield 65% and mp 83 °C. IR (KBr pellet, cm^{-1}): 1641.4 and 1469.6 (Ar CH and CN), ^1H NMR ($CDCl_3$, 400 MHz) δ: 9.35 (d, 2H, Py CH, *J* 6.6 Hz), 7.91 (d, 2H, Py CH, *J* 6.3 Hz), 4.92 (t, 2H, Py$-CH_2-$, *J* 7.4 Hz), 2.68 (s, 3H, CH_3-), 2.01 (q, 2H, $-CH_2-$), 1.33 (q, 4H, $-CH_2-$), 1.23 (q, 6H, $-CH_2-$), 0.86 (t, 3H, $-CH_3$, *J* 6.6 Hz).

*2.2.2.3. 4-Methyl-N-n-dodecyl pyridinium bromide (**1c**).* Yield 83% and mp 41 °C. IR (KBr pellet, cm^{-1}): 1640.4 and 1468.2 (Ar CH and CN), ^1H NMR ($CDCl_3$, 400 MHz) δ: 9.24 (d, 2H, Py CH, *J* 6.4 Hz), 7.88 (d, 2H, Py CH, *J* 5.2 Hz), 4.90 (t, 2H, Py$-CH_2-$, *J* 14 Hz), 2.68 (s, 3H, CH_3-), 1.99 (q, 4H, $-CH_2-$), 1.32 (q, 2H, $-CH_2-$), 1.23 (q, 6H), 0.87 (t, 3H, $-CH_3$, *J* 5.1 Hz).

2.2.3. Synthesis of DHEASPI-C_1, DHEASPBr-C_8 and DHEASPBr-C_{12}

With a catalytic amount of piperidine, three dyes were synthesized by the reaction of 4-(*N*,*N*-diethanolanilino) benzaldehyde with compounds **1a**–**1c**.

2.2.3.1. trans-4-[p-(N,N-Di (2-hydroxyethyl))-amino-styryl]-N-methyl pyridinium iodide (DHEASPI-C_1). A mixture of compound **3** (2.09 g, 0.01 mol) and **1a** (2.35 g, 0.01 mol) was stirred in methanol (25 mL) at reflux temperature overnight in the presence of 4–5 drops of piperidine. After removal of the solvent, crude product (DHEASPI-C_1) was produced and

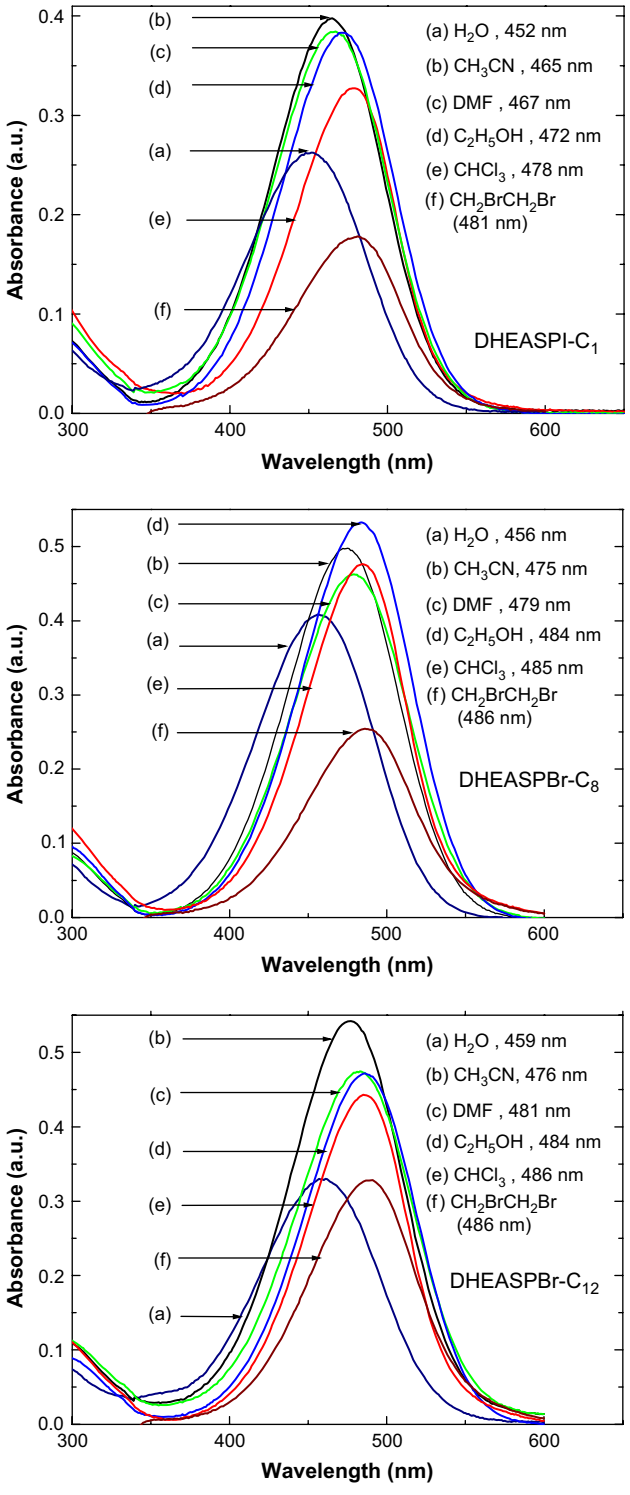

Fig. 1. Linear absorption spectra of DHEASPI-C_1, DHEASPBr-C_8 and DHEASPBr-C_{12} in different solvents at $d_0 = 1 \times 10^{-5}$ mol/L.

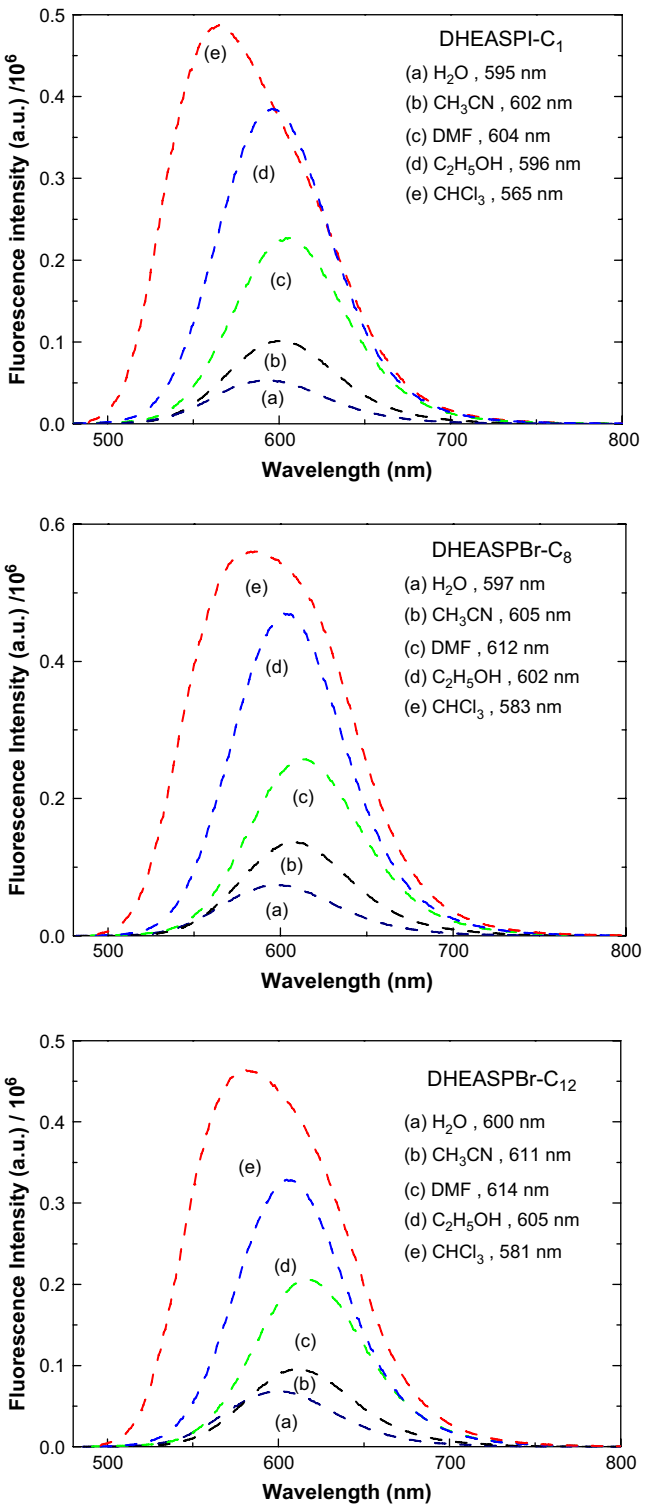

Fig. 2. Single-photon fluorescence spectra (dash) of DHEASPI-C_1, DHEASPBr-C_8 and DHEASPBr-C_{12} in different solvents at $d_0 = 1 \times 10^{-5}$ mol/L.

purified by column chromatography on silica gel using ethanol as eluent.

Yield 73% and T_d 306.5 °C. The crude product was purified by column chromatography on silica gel using ethanol as eluent. ^{1}H NMR (DMSO-d_6, 400 MHz) δ: 8.64 (2H, Py–CH, d, J 6.4 Hz), 8.02 (2H, Py–CH, d, J 6.4 Hz), 7.87 (1H, CH=CH, d, J 14.2 Hz), 7.59 (2H, Ar-H, d, J 7.6 Hz), 7.17 (1H, CH=CH, d, J 15.6 Hz), 6.88 (2H, Ar-H, d, J 7.8 Hz), 4.18–4.16 (5H, d, J 4.0 Hz), 3.68 (8H, $-CH_2-$, q). Elemental

analysis: calcd C, 50.71; H, 5.44; N, 6.57. Found: C, 50.46; H, 5.38; N, 6.02.

2.2.3.2. trans-4-[p-(N,N-Di (2-hydroxyethyl))-amino-styryl]-N-octyl pyridinium bromide (DHEASPBr-C_8). A mixture of compound **3** (3.14 g, 0.015 mol) and **1b** (4.28 g, 0.015 mol) was stirred in methanol (50 mL) at reflux temperature overnight in the presence of 4–5 drops of piperidine. After removal of the solvent, crude product (DHEASPBr-C_8) was produced and purified by column chromatography on silica gel using ethanol as eluent.

Yield 69% and T_d 298.0 °C. The crude product was purified by column chromatography on silica gel using ethanol as eluent. ^{1}H NMR (DMSO-d_6, 400 MHz) δ: 8.80 (2H, Py–CH, d, J 6.9 Hz), 8.08 (2H, Py–CH, d, J 6.6 Hz), 7.92 (1H, CH=CH, d, J 15.9 Hz), 7.58 (2H, Ar-H, d, J 9.0 Hz), 7.16 (1H, CH=CH, d, J 16.2 Hz), 6.81 (2H, Ar-H, d, J 9.0 Hz), 4.44 (2H, Py–CH_2–, t, J 7.5 Hz), 3.55 (8H, –CH_2–, q), 1.27–1.24 (10H, –CH_2–, q), 1.16 (2H, –CH_2–, q), 0.85 (3H, –CH_3, t, J 7.05 Hz). Elemental analysis: calcd C, 62.89; H, 7.81; N, 5.87. Found: C, 62.48; H, 7.57; N, 5.56.

2.2.3.3. trans-4-[p-(N,N-Di (2-hydroxyethyl))-amino-styryl]-N-dodecyl pyridinium bromide (DHEASPBr-C_{12}). A mixture of compound **3** (2.09 g, 0.01 mol) and **1c** (3.41 g, 0.01 mol) was stirred in methanol (30 mL) at reflux temperature overnight in the presence of 4–5 drops of piperidine. After removal of the solvent, crude product (DHEASPBr-C_{12}) was produced and purified by column chromatography on silica gel using ethanol as eluent.

Yield 72% and T_d 275.5 °C. The crude product was purified by column chromatography on silica gel using ethanol as eluent. ^{1}H NMR (DMSO-d_6, 400 MHz) δ: 8.72 (2H, Py–CH, d, J 6.4 Hz), 8.02 (2H, Py–CH, d, J 6.4 Hz), 7.88 (1H, CH=CH, d, J 16.0 Hz), 7.56 (2H, Ar-H, d, J 8.4 Hz), 7.12 (1H, CH=CH, d, J 16.0 Hz), 6.79 (2H, Ar-H, d, J 8.8 Hz), 4.39 (2H, Py–CH_2–, t, J 6.8 Hz), 3.56 (8H, –CH_2–, q), 1.86 (2H, –CH_2–, q), 1.25–1.21 (18H, –CH_2–, q), 0.83 (3H, –CH_3, t, J 6.6 Hz). Elemental analysis: calcd C, 65.27; H, 8.50; N, 5.25. Found: C, 65.09; H, 8.11; N, 5.03.

3. Results and discussion

In this paper, we investigated the influence of styryl-pyridinium salts upon TPA behaviors, where *N*-phenyldiethanolamine group acted as donor and different terminal substituted pyridinium groups as acceptors.

Fig. 1 shows the linear absorption spectra of three dyes in different solvents. One can see that the absorption properties of the three dyes are greatly influenced by the solvents used, that is, peak locations are blue-shifted with the increase of the solvent polarity parameter (ε [23]). For example, the maximum absorption peak for DHEASPI-C_1 in Fig. 1(a) is at 481 nm in CH_2BrCH_2Br (ε, 4.76), 478 nm in $CHCl_3$ (ε, 4.9), 472 nm in ethanol (ε, 25.7), 467 nm in DMF (ε, 36.71), 465 nm in CH_3CN (ε, 37.5) and 452 nm in H_2O (ε, 80.1). Similar solvent effect for DHEASPBr-C_8 and DHEASPBr-C_{12} is shown in Fig. 1(b) and (c). The short wavelength absorption maximum is attributed to the molecular structure of dye. The three dyes (DHEASPI-C_1, DHEASPBr-C_8 and DHEASPBr-C_{12}) investigated in this paper are pyridinium salts containing character cations and anions, so they can easily form stable complex with polar solvent in ground state for electrostatic attraction and the energy difference (ΔE) of HOMO–LUMO increase, then $\pi \rightarrow \pi^*$ transition inclines to blue shift with the increase of ε.

Table 1
The fluorescence quantum yields (Φ_f) of DHEASPI-C_1, DHEASPBr-C_8 and DHEASPBr-C_{12} in different solvents at $d_0 = 1 \times 10^{-5}$ mol/L

	H_2O (ε, 80.1)	CH_3CN (ε, 37.5)	DMF (ε, 36.71)	Ethanol (ε, 25.7)	$CHCl_3$ (ε, 4.9)
DHEASPI-C_1	0.112	0.139	0.373	0.574	1.145
DHEASPBr-C_8	0.101	0.149	0.354	0.504	0.998
DHEASPBr-C_{12}	0.114	0.095	0.275	0.393	0.859

The absorptivity in DMF (or CH_3CN) is two orders of magnitude higher than that in CH_2BrCH_2Br in Fig. 1. This is related to the dyes' poor solubility in this solvent in the measurement of UV–vis absorption spectra, so absorption spectra were weak.

Fig. 2 shows the single-photon fluorescence spectra for the three dyes in different solvents. It is easily seen that, with solvent polarity parameter (ε) increase, both the fluorescence intensity and fluorescence quantum yield (Φ_f) (shown in Table 1) of the three dyes decreased. This can be explained by the "twisted intra-molecular charge transfer" (TICT) model [25], shown in Fig. 3. According to the TICT model and Fig. 4, larger the solvent polarity, more obvious the solvation for the non-emissive "TICT" state, so the dye gives very low fluorescence intensity in higher polar solvent. The similar effect was observed in DEASPS and HEASPI [20,21].

One can also see that the fluorescence quantum yield datum (Φ_f) in chloroform is the biggest and that of dye C_1 is 1.145, i.e. higher than 1. Part of the reason is the dye's poor solubility in chloroform, especially for DHEASPI-C_1, thus the absorbance in UV-absorption spectrum was lower. On the other hand, the complex of dyes and solvent decreases its UV-absorption intensity too. Therefore, we present Φ_f in more polar solvent for dye C_1, which are all less than 1. When Φ_f of the three dyes were compared, one can see that the value inclined to decrease as alkyl chain length increased especially when polarity parameter (ε) was less high, while changed a little in DMF and CH_3CN for solvent quenching effect.

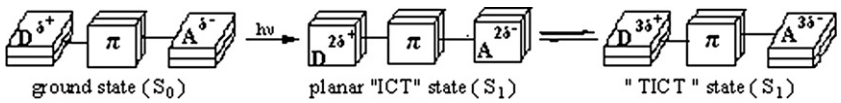

Fig. 3. Charge transfer "TICT" model.

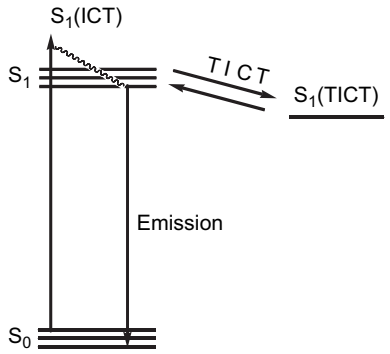

Fig. 4. The micro-process of the one-photon fluorescence.

Interestingly, one can also see that the three fluorescence spectra incline to red shift as solvent dipole moments ($\mu/10^{-30}$ C m [23]) increase, as for DHEASPBr-C_8, from 583 nm ($CHCl_3$, μ, 3.84) to 602 nm (ethanol, μ, 5.6), to 597 nm (H_2O, μ, 6.47), to 605 nm (CH_3CN, μ, 11.47), to 612 nm (DMF, μ, 12.88). That are like PSPI mentioned before, its predicated dipole moments obtained by PM3 calculations confirm that the dipole moment of PSPI in the excited state greater than that in the ground state by 3.4 D [20]. Here, the dipole moment of dye in the excited state is also greater than that in the ground state, which can be certified by the Lippert–Mataga equation [24] (Fig. 5).

$$hc(\nu_{abs} - \nu_{em}) = \frac{1}{4\pi\epsilon_0}\frac{2}{\alpha^3}\mu_e(\mu_e - \mu_g)\Delta f + \text{const}$$

$$\Delta f = \frac{\epsilon - 1}{2\epsilon + 1} - \frac{(n^2 - 1)}{(2n^2 + 1)}$$

where, μ_e and μ_g are the dipole moments in the excited and ground states, respectively. $(\nu_{abs} - \nu_{em})$ is Stokes shift. ε is the dielectric constant and n is the optical refractive index.

One can see that the slopes are all larger than zero, then μ_e is larger than μ_g. As a result, the fluorescence spectra of dyes are red-shifted with the increase of the solvent dipole moment (μ).

From Figs. 1 and 2, one can see that the location of spectra of DHEASPBr-C_8 or DHEASPBr-C_{12} is almost around 490 nm (absorption) and 582 nm (fluorescence) except that DHEASPI-C_1 is located at 480 nm (absorption) and 565 nm (fluorescence). The result is due to σ-configuration effect of the alkyl group in pyridinium terminal acceptor when it changes from methyl to octyl, and to dodecyl. But when the spectral intensity of the three dyes is concerned, the change is special. This can also be explained by TICT model. When the alkyl group in pyridinium terminal acceptor changes from methyl to octyl, the molecular structure becomes harder and fluorescence increases a lot. But when it changes from octyl to dodecyl, the combined carbon chain is too long to twist itself and the fluorescence intensity declines too.

For further explanation on TICT model, β-cyclodextrin (β-CD) was added into different dye solutions and all the

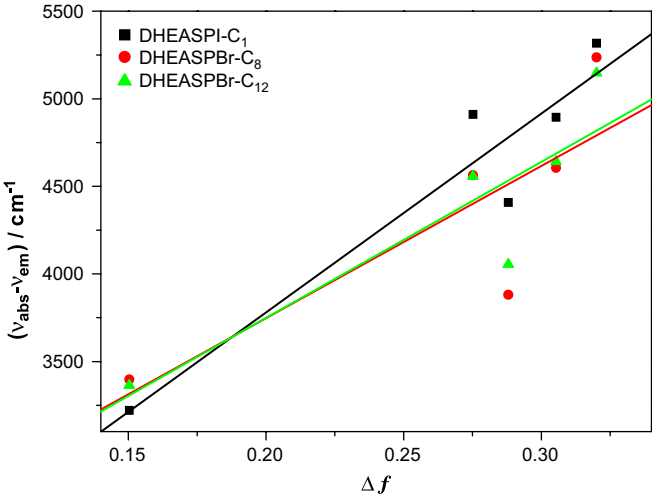

Fig. 5. The Lippert–Mataga plot for the three dyes.

single-photon fluorescence intensities were increased, as shown in Fig. 6.

As shown in Fig. 7, DHEASPI-C_1 was surrounded by 10 000 times β-CD and it cannot twist easily, so the planarity of the dye was improved and fluorescence intensity increased. At the same time, there were about 3–6 nm blue shifts when β-CD was added into different dyes. However, when the alkyl group in pyridinium terminal acceptor changes from methyl to octyl and to dodecyl, molecular is difficult to enter β-CD for the bulk resistance effect. So β-CD has little influence on DHEASPBr-C_8 and DHEASPBr-C_{12}.

Fig. 8 shows the TPA induced fluorescence spectrum of the three dyes in DMF solution with 1 cm path length and a concentration of 0.001 mol/L when pumped by using 1064 nm laser beam. It can be seen that the wavelengths are 613 nm for DHEASPI-C_1, 620 nm for DHEASPBr-C_8 and 624 nm for DHEASPBr-C_{12}. When the two-photon absorption cross-section (σ_s) was calculated and that of DHEASPI-C_1 was the

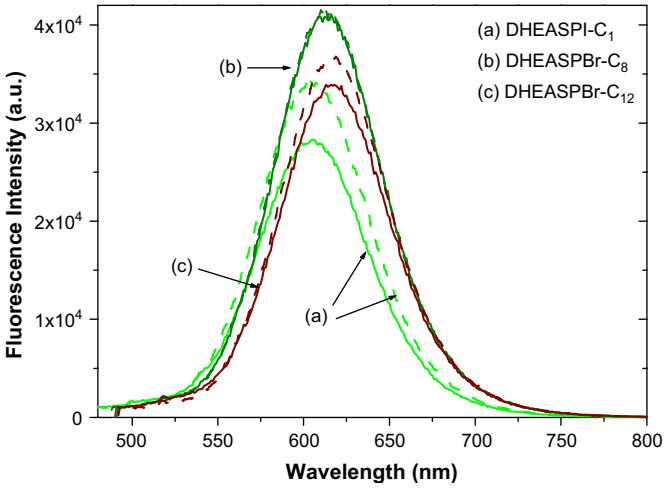

Fig. 6. Single-photon fluorescence spectra of pure dye (solid) and dye + β-CD (dash) in DMF solvent at d_0 (dye) = 1×10^{-6} mol/L and d_0 (β-CD) = 1×10^{-2} mol/L.

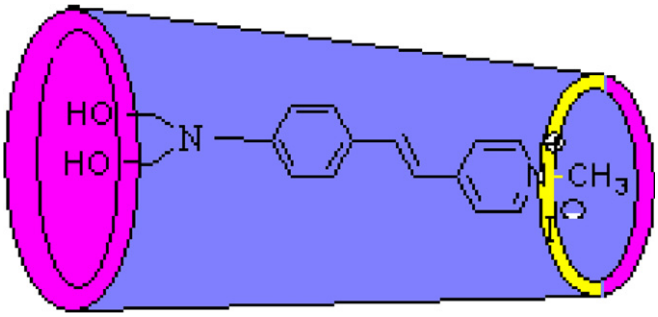

Fig. 7. The ideal sketch of DHEASPI-C_1 molecule structure when surrounded by β-CD in DMF solvent.

reference, σ_s of DHEASPBr-C_8 and DHEASPBr-C_{12} are 8.02 times and 13.5 times, respectively. This is an obvious red shift and the σ_s increases a lot with the increase of carbon number in alkyl group. This is related to the σ-configuration effect of the alkyl group in pyridinium terminal acceptor.

Comparing Fig. 8 with Fig. 2, there is about 8–10 nm red shift for the peak of TPA induced fluorescence spectrum compared with that of the single-photon induced fluorescence spectrum. This can be explained by re-absorption effect. As mentioned before [26], there is an overlap between linear absorption spectrum and single-photon induced fluorescence spectrum, and the overlap will enlarge as the concentration becomes higher. The single-photon induced fluorescence spectrum was measured at a very low concentration ($d_0 = 1 \times 10^{-5}$ mol/L), and the re-absorption effect can be neglected. But the TPA induced fluorescence spectrum was measured at a higher concentration (0.001 mol/L), the re-absorption effect greatly decreases the blue side of the TPA induced fluorescence spectrum.

4. Conclusions

We have synthesized three "D–π–A" stilbene-type dyes that display good linear absorption and single-photon fluorescence properties as well as excellent thermal stability. Owing to the different pyridinium terminal acceptors, their electron-donating abilities are different. There is a red shift in both one-photon and two-photon fluorescence spectra from DHEASPI-C_1 to DHEASPBr-C_8 and to DHEASPBr-C_{12} as the alkyl group in pyridinium terminal acceptor changes from methyl to octyl and to dodecyl. As far as solvent influence is concerned, all the absorption spectra are blue-shifted with the increase of the solvent polarity parameter (ε), and there is an obvious decrease in fluorescence intensity and Φ_f at the same time. On the other hand, the fluorescence spectra incline to red shift as solvent dipole moment (μ) increases. As far as the two-photon excited fluorescence spectra are concerned, their peak locations are 613 nm, 620 nm, and 624 nm, respectively. When DHEASPI-C_1 was the reference, two-photon absorption cross-sections (σ_s) of DHEASPBr-C_8 and DHEASPBr-C_{12} are 8.02 times and 13.5 times, respectively.

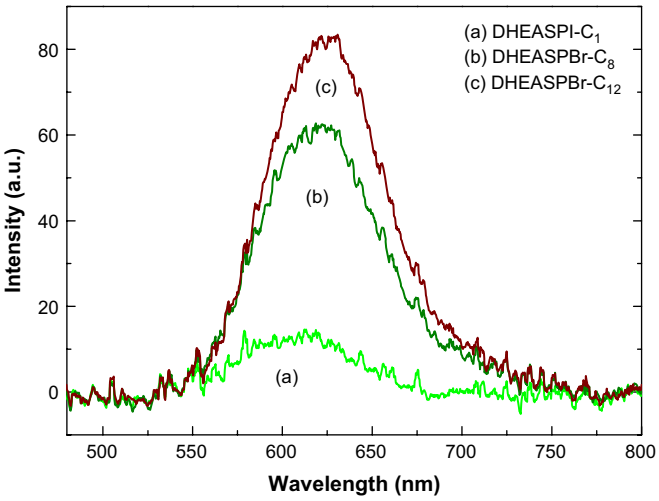

Fig. 8. Two-photon induced fluorescence spectra of DHEASPI-C_1, DHEASPBr-C_8 and DHEASPBr-C_{12} in DMF solvent at $d_0 = 0.001$ mol/L.

Acknowledgements

The authors are grateful to the National Natural Science Foundation of China (Grant Nos. 50673071 and 50673020) and the Foundation for the Author of National Excellent Doctoral Dissertation of PR China (FANEDD, Grant No. 200333) for financial support.

References

[1] Bhawalkar JD, He GS, Park CK, Zhao CF, Ruland G, Prasad PN. Opt Commun 1996;124:33.
[2] Ehrlich JE, Wu XL, Lee I-YS, Rckel H, Marder SR, Perry JW. Opt Lett 1997;22:1843.
[3] He Guang S, Lixiang Yuan, Prasad Paras N, Abbotto A, Facchetti A, Pagani GA. Opt Commun 1997;140:49.
[4] Bhawalkar JD, Kumar ND, Zhao CF, Park CK, Ruland G, Prasad PN. Laser Med Surg 1997;15:201.
[5] He GS, Xu GC, Prasad PN, Reinhardt BA, Bhatt JC, McKellar R, et al. Opt Lett 1995;20:435.
[6] Cumpston Brian H, Ananthavel Sundaravel P, Stephen Barlow, Dyer DL, Ehrlich JE, Erskine LL, et al. Nature 1999;398:51.
[7] Parthenopoulos DA, Rentzepis PM. Science 1989;245:843.
[8] Dvornikov AS, Liang Y, Cruse CS, Rentzepis PM. J Phys Chem B 2004;108:8652.
[9] Maruo S, Nakamura O, Kawata S. Opt Lett 1997;22:132.
[10] Zhao YX, Li X, Wu FP, Fang XY. J. Photochem Photobiol A: Chem 2006;177:12.
[11] Huang ZZ, Wang XM, Li B, Lv CG, Xu J, Jiang WL. Opt Mater 2007;29:1084.
[12] Schafer KJ, Hales JM, Balu M, Belfield KD, Van Stryland EW, Hagan DJ. Photobiol A: Chem 2004;162:497.
[13] Yoo J, Yang SK, Jeong M-Y, Ahn HC, Jeon S-J, Cho BR. Org Lett 2003;5:645.
[14] Drobizhev M, Karotki A, Dzenis Y, Rebane A, Suo Z, Spangler CW. J Phys Chem B 2003;107:7540.
[15] Zhang BJ, Jeon S-J. Chem Phys Lett 2003;377:210.
[16] Lee HJ, Sohn J, Hwang J, Park SY, Choi H, Cha M. Chem Mater 2004;16:456.
[17] He GS, Cui Y, Bhawalkar JD, Prasad PN, Bhawalkar DD. Opt Commun 1997;133:175.
[18] He GS, Yuan LX, Cui Y, Li M, Prasad PN. J Appl Phys 1997;81:2529.

[19] Wang XM, Zhou YF, Yu WT, Wang C, Fang Q, Jiang ML, et al. J Mater Chem 2000;10:2698.
[20] Wang XM, Wang D, Zhou GY, Yu WT, Zhou YF, Fang Q, et al. J Mater Chem 2001;11:1600.
[21] Wang XM, Wang D, Jiang WL, Jiang MH. Opt Mater 2002;20:217.
[22] Wang XM, Zhou YF, Wang C, Jiang M, Zhao X, Jiang MH, et al. Science in China (E) 2002;32:20.
[23] Cheng NL. Solvents handbook. Third version. Chemistry Industry Press; 2002. p. 198, 305, 711, 817, 981.
[24] Krebs FC, Spanggaard H. J Org Chem 2002;67:7185.
[25] Sarkar N, Das K, Nath DN, Bhattacharyya K. Langmuir 1994;10: 326.
[26] Zhuo GY, Wang XM, Wang D, Wang C, Zhao X, Shao ZS, et al. Optics & Laser Technology 2001;33:209.